Stability of Hyperlithiated Borides

Kiet A. Nguyen,[†,‡] G. Naga Srinivas,[†] Tracy P. Hamilton,[†] and Koop Lammertsma*[,†,§]

Department of Chemistry, University of Alabama at Birmingham, Birmingham, Alabama 35294, and Faculty Sciences, Department of Chemistry, Vrije Universiteit, De Boelelaan 1083, 1081 HV Amsterdam, The Netherlands

Received: October 23, 1998

Structures and energetics of BLi_n ($n = 4-8$) clusters are predicted using the SCF, MP2, and B3LYP methods with the 6-31G(d) basis set, including energy evaluations at G2MP2. Cohesive energies, defined as the enthalpies of the $BLi_n \rightarrow B + Li_n$ reactions, and Li and Li_2 elimination reaction enthalpies are also estimated at B3LYP. This level of theory predicts the boron cohesive energy to increase up to the BLi_6 cluster after which it levels off. All BLi_n systems are thermodynamically stable with respect to Li and Li_2 dissociations; BLi_4 has the largest reaction enthalpies. The energetics of the hyperlithiated borides obtained with B3LYP/6-31G(d) are in reasonable agreement with those at G2MP2 but less satisfactory than those of the smaller BLi_n ($n = 1-3$) systems. Computations on BLi_4 with multiconfigurational quasidegenerate perturbation theory indicate that the B3LYP/6-31G(d) energies may be more reliable for the larger BLi_n systems.

I. Introduction

Lithium atoms are known to form hypervalent compounds with group 13−17 elements of the periodic table. Structures and energetics for many of these hyperlithiated compounds have been reported in theoretical studies.[1−4] Some have been studied experimentally such as, for example, OLi_4 and OLi_5, which were detected by Wu.[5] The hyperlithiated carbide CLi_6 was observed in 1992 by Kudo[6] a decade after Schleyer et al.[3] predicted its possible existence. Recent theoretical data of Ivanic and Marsden suggest the even larger polylithiated carbon clusters CLi_8, CLi_{10}, and CLi_{12} to be of reasonable stability.[7]

In contrast to the well-studied hyperlithiated carbides, theoretical studies of similarly sized and larger boron−lithium systems have been limited to the work of Meden et al.[8] They computed structures and energetics at the SCF/6-31G(d) level to evaluate the formation of a Li_3B compound in the dissolution of crystalline boron in the lithium melt. Partly on the basis of computed cohesive energies, they argued that boron does not dissolve completely in molten lithium. Although these SCF structures are informative, "electron-deficient" systems are known to require correlated methods for acceptable estimates of structural parameters and energies. In a recent systematic study, we demonstrated the importance of the effects of electron correlation in accurately characterizing stationary points on the potential energy surface (PES) of small BLi_n ($n = 1-3$) systems.[9]

To shed more light on hyperlithiated borides and to assist in their gas-phase detection, we now report ab initio calculations on BLi_n ($n = 4-8$) to examine their structures and thermal stabilities. In particular, we gauge the $BLi_n \rightarrow B + Li_n$ reaction, which measures the stabilization (i.e., cohesive energy) that a boron atom provides to the BLi_n clusters. To explore the thermodynamic driving force for the Li and Li_2 elimination channels, reaction enthalpies for $BLi_n \rightarrow BLi_{n-1} + Li$ and $BLi_n \rightarrow BLi_{n-2} + Li_2$ are reported for ground-state processes.

II. Computational Methods

All electronic structure calculations were carried out using the GAUSSIAN 94 suite of programs.[10] The structures of all BLi_n isomers were calculated at the Hartree−Fock (HF) self-consistent field (SCF) level,[11,12] Møller−Plesset second-order perturbation theory (MP2),[13,14] and Kohn−Sham theory[15] using the 6-31G(d)[16] basis set. For the density functional theory (DFT) calculations we used Becke's three-parameter hybrid exchange functional combined with the Lee−Yang−Parr correlation functional,[17−19] hereafter referred to as B3LYP. The structures were verified to be either minima or transition structures by evaluating the second derivatives of the energy (Hessian matrix).

Enthalpies of formation are estimated at G2MP2. This method[20] uses MP2/6-31G(d) geometries and obtains its energies from the QCISD(T) method,[21] using the 6-311G(d,p) basis set,[22] with basis set additivity corrections at the MP2 level of theory. The combination of basis set and correlation corrections, and two empirical corrections yields

$$E(\text{G2MP2}) = E(\text{QCISD(T)/6-311G(d,p)}) + E(\text{MP2/6-311+G(3df,2p)}) - E(\text{MP2/6-311G(d,p)}) + E(\text{HLC}) + E(\text{ZPE})$$

where the empirical "higher level correction" is given by $E(\text{HLC}) = (-0.19n\alpha - 4.81n\beta) \times 10^{-3}$ au. $E(\text{ZPE})$ is obtained by scaling the SCF/6-31G(d) harmonic frequencies by 0.8929. For 125 experimental energies, the G2MP2 method is reported to give a mean absolute deviation of 1.58 kcal/mol.[20,23] Kohn−Sham DFT with B3LYP functionals also delivers impressive thermochemical accuracy with a mean absolute deviation of 2.4 kcal/mol for a similar test set that includes 110 experimental energies.[17] Although numerous examples show B3LYP results to compare favorably with high levels of theory and with experiments, such comparisons for boron−lithium systems are limited to only the computed small BLi_n ($n = 1-3$) clusters owing to the absence of experimental data. For these clusters

* Address correspondence to the author at the address in The Netherlands.
† University of Alabama at Birmingham.
‡ Current address: Air Force Research Laboratory, Materials Directorate, AFRL/MLPJ, Wright-Patterson AFB, Dayton, Ohio 45433.
§ Vrije Universiteit.

10.1021/jp984160x CCC: $18.00
Published on Web 01/23/1999

the DFT geometries and energetics are in excellent agreement with high levels of theory.[9]

Owing to the proximity of the potential energy surfaces of excited states for some of the open-shell systems considered here, HF and HF-based correlated calculations may exhibit multiple solutions that are associated with the same symmetry and electronic configuration. For example, at MP2/6-31G(d), two $^2A_{2u}$ states are found for the D_{4h} form of BLi_4 with one exhibiting more spin contamination than the other. In this and in other cases data are reported for the lowest energy and the least spin-contaminated state.

Given the uncertainty in the accuracy of the energies for highly spin-contaminated molecules, we used the GAMESS[24] program to perform complete active space SCF calculations with seven electrons in seven active orbitals (CASSCF(7,7)) for the BLi_4 isomers (i.e.,geometry optimizations and frequencies analyses) followed by multiconfigurational quasidegenerate second-order perturbation theory (MCQDPT2)[25] for higher accuracy in the energies. However, throughout B3LYP will be used for all final energy evaluations of the BLi_n systems.

III. Results and Discussion

Structures of BLi_n ($n = 4-8$) with B3LYP geometrical parameters are displayed in Figure 1 with MP2 values in brackets and those at SCF in parentheses. The geometrical data of these structures, computed with the three methods, compare reasonably well. The average BLi bond length for all systems is 2.170 ± 0.043 Å at MP2, while slightly shorter at B3LYP (2.137 ± 0.051 Å) and comparably longer at SCF (2.217 ± 0.061 Å). More noticeable deviations in some of the structures are due to the flatness of the potential energy surface compounded by the effect of electron correlation. Not surprisingly, CASSCF(7,7) tends to predict longer bonds for BLi_4 (shown in italics in Figure 1).

Total and relative energies are tabulated in Tables 1 and 2 for all BLi_n and Li_n ($n = 4-8$) systems. Table 3 lists the BLi_n boron cohesive energies, defined as the enthalpy for the $BLi_n \rightarrow B + Li_n$ reaction. Tables 4 and 5 give respectively the Li and Li_2 elimination energetics for BLi_n, and the corresponding ones for Li_n are listed for comparison in Tables 6 and 7. Thermodynamic data for BLi, BLi_2, and BLi_3 are included in Tables 3−5, also for comparison. The enthalpies given in these tables include zero-point energy corrections except for Table 1, which lists absolute energies.

As expected, only for a few BLi_n systems do the SCF and MP2 energetics show reasonable agreement with those at G2MP2, which is the highest level of theory we employ. Deviations from the G2MP2 energies for the Li-elimination reactions (Table 4) are as large as 40 and 27 kcal/mol for SCF and MP2, respectively. The differences between B3LYP and G2MP2 are less pronounced but remain significant (up to 15 kcal/mol), in contrast to those found for the smaller BLi_n ($n = 1-3$) systems. Whereas the overall trends in energetics predicted by both B3LYP and MP2 are consistent with those at G2MP2, this, however, is not the case for SCF. The SCF performance is particularly poor for the $B-Li_n$ cohesive energies listed in Table 3.

In the following subsections, we discuss for each BLi_n cluster their structural features and energetics with emphasis on the most stable forms. Unless noted otherwise, B3LYP data are used.

A. BLi_4. Five BLi_4 structures were identified with C_{2v}, D_{2d}, C_{4v}, D_{4h}, and T_d symmetry (Figure 1). Of these only the C_{2v} and D_{2d} structures are minima at all levels of theory. At the

TABLE 1: Total (au) and Relative (kcal/mol) Energies for BLi_n Systems[a]

str/sym/level	energy	$\langle S^2 \rangle$	rel energy	NIF (cm^{-1})
	(a) BLi_4			
D_{2d} ($^2B_2$)				
B3LYP	−54.838 87	0.961	0	0
SCF	−54.355 20	2.264	0	0
MP2	−54.476 06	2.173	0	0
G2MP2[b]	−54.583 58		0	
CASSCF(7,7)	−54.406 16		0	0
MCQDPT2	−54.501 73		0	
C_{2v} ($^2B_2$)				
B3LYP	−54.836 00	0.767	1.8	0
SCF	−54.376 38	1.772	−13.3	0
MP2	−54.478 72	1.737	−1.6	0
G2MP2[b]	−54.558 40		15.8	
CASSCF(7,7)	−54.408 35		−1.3	0
MCQDPT2	−54.504 85		−2.0	
D_{4h} ($^2A_{2u}$)				
B3LYP	−54.838 45	0.767	0.2	1 (48i)
SCF	−54.339 52	0.776	9.4	2 (265i, 71i)
MP2	−54.496 99	0.776	−14.5	2 (312i, 20i)
G2MP2	−54.563 56		12.6	
CASSCF(7,7)	−54.404 18		1.2	0
MCQDPT2	−54.500 38		0.8	
C_{4v} ($^2A_1$)				
B3LYP	−54.838 45	0.767	0.2	1 (47i)
SCF	−54.340 74	0.767	8.7	1 (44i)
MP2	−54.497 30	0.767	−13.2	1 (44i)
G2MP2	−54.563 46		12.6	
CASSCF(7,7)	−54.404 86		0.8	0
MCQDPT2	−54.500 64		0.7	
T_d				
B3LYP	−54.827 12	0.764	6.5	2 (1924i, 1923i)
	(b) BLi_5			
C_{4v}				
B3LYP	−62.401 05		0	0
SCF	−61.809 90		0	0
MP2	−62.015 46		0	0
G2MP2	−62.080 67		0	
D_{3h}				
B3LYP	−62.397 93		1.4	2 (54i, 54i)
SCF	−61.805 56		2.5	2 (40i, 40i)
MP2	−62.013 72		0.6	2 (13i, 13i)
G2MP2	−62.078 00		1.7	
C_{2v}				
B3LYP	−62.397 95		1.5	1 (90i)
SCF	−61.805 56		2.6	1 (67i)
MP2	−62.013 72		0.7	1 (26i)
G2MP2	−62.077 91		1.7	
	(c) BLi_6			
O_h ($^2A_{1g}$)				
B3LYP	−69.962 79	0.769		0
SCF	−69.316 42	1.936		0
MP2	−69.489 71	1.865		0
G2MP2	−69.581 83			
	(d) BLi_7			
D_{5h}				
B3LYP	−77.492 94		0.0	0
SCF	−76.740 33		0.0	0
MP2	−76.997 90		0.0	0
G2MP2	−77.067 38		0.0	
C_{3v} (staggered)				
B3LYP	−77.486 94		3.8	0
SCF	−76.740 01		0.2	0
MP2	−76.985 80		7.7	0
G2MP2	−77.061 58		3.6	0
C_{3v} (ecllipsed)				
B3LYP	−77.473 00		12.4	1 (116i)
SCF	−76.724 81		9.5	1 (123i)
MP2	−76.967 06		19.1	1 (132i)
G2MP2	−77.048 02		12.1	
	(e) BLi_8			
C_{3v}				
B3LYP	−85.004 21[b]	0.792	0.0	0
SCF	−84.204 83[b]	1.645	0.0	2 (111i, 111i)
MP2	−84.413 36[b]	1.507	0.0	
G2MP2				
D_{4h} ($^2A_{2u}$)				
SCF	−84.159 39	1.988	26.6	

[a] Using the 6-31G(d) basis set. Relative energies include zero-point energy corrections. NIF = number of imaginary frequencies. [b] Symmetry-broken solutions for the D_{2d} ($^2B_2$) form of BLi_4 at MP2/6-311+G(3df,2p).

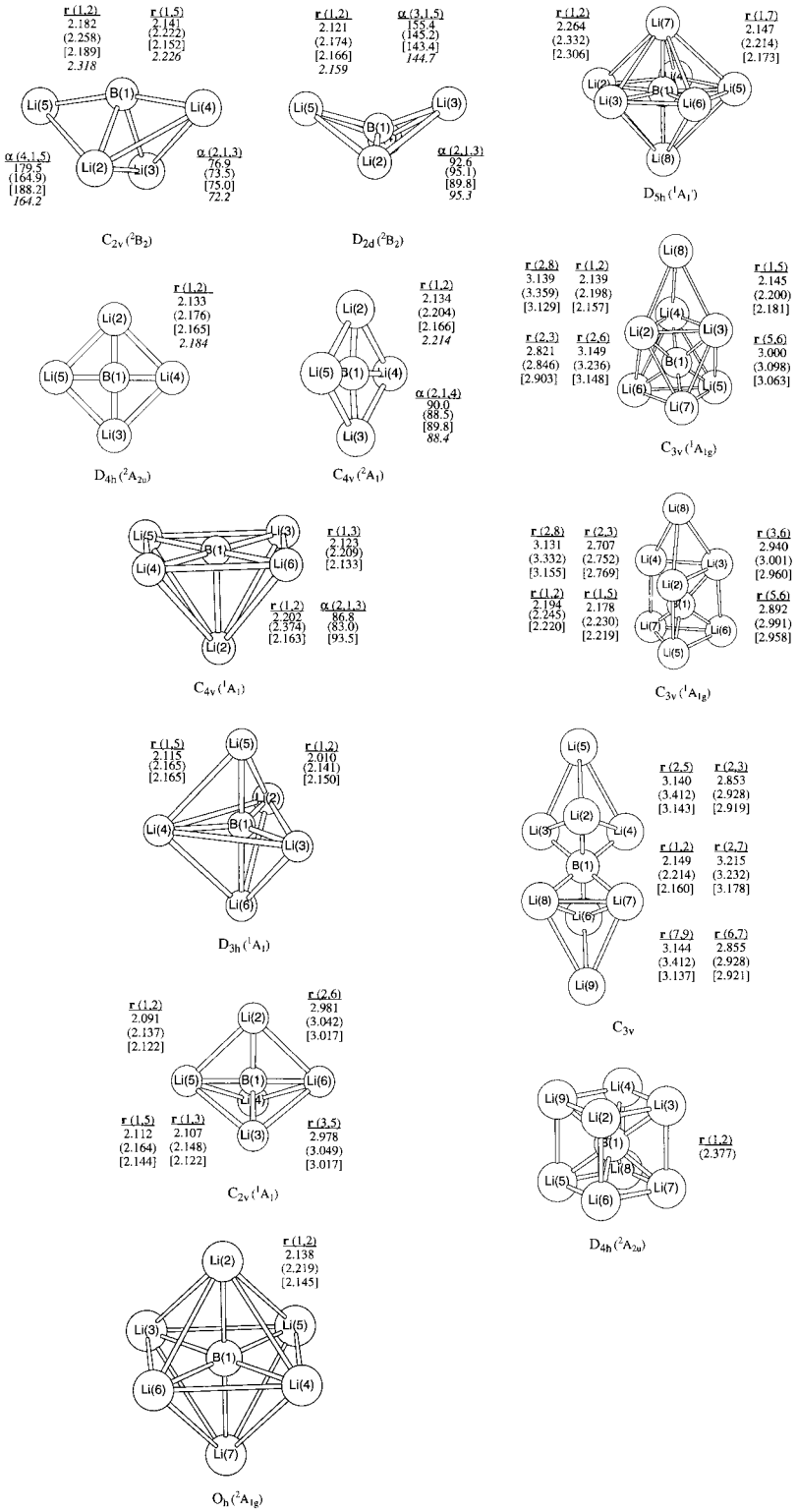

Figure 1. BLi_n ($n = 4-8$) structures with geometrical parameters at B3LYP, MP2 (in brackets), and SCF (in parentheses) with the 6-31G(d) basis set. The CASSCF(7,7) distances and angles for BLi_4 are in italics.

MP2 level the D_{2d} structure has a B−Li bond length of 2.166 Å and a large Li−B−Li angle of 143°. The C_{2v} structure, which can be viewed as a bi-Li-capped BLi_2 ring, is the only one with Li_3 triangular interactions (a common motif in lithium clusters). None of the C_{4v}, D_{4h}, and T_d forms, which are the only BLi_4 structures reported by Meden et al.,[8] are minima at SCF or at B3LYP. The C_{4v} isomer is a transition structure at all levels with normal modes leading to the D_{2d} structure. Note that the C_{4v} form is actually planar at B3LYP, thus having D_{4h} symmetry. This D_{4h} structure has two imaginary frequencies at SCF and MP2 with normal modes leading to the C_{4v} and D_{2d} structures. The T_d form is a "hill-top" structure at B3LYP, at which level it has a symmetry-broken solution. Its two degenerate frequencies have normal modes leading to the D_{2d} structure.

B3LYP predicts the C_{2v} and D_{2d} forms to be nearly isoenergetic with a 1.8 kcal/mol preference for the D_{2d} isomers, while both CASSCF(7,7) and MCQDPT2 give a similar small energy difference in favor of the C_{2v} isomer as does MP2. Interestingly, G2MP2 estimates the C_{2v} to be less stable by a sizable 15.8 kcal/mol. B3LYP, CASSCF(7,7), and MCQDPT2 also predict

TABLE 2: Total (au) and Atomization (kcal/mol) Energies for Li_n Systems[a]

level	Li_4 (D_{2h})	Li_5(C_{2v})	Li_6 (D_{3h})	Li_7 (D_{5h})	Li_8 (T_d)
			Total Energy		
B3LYP	−30.053 97	−37.574 20	−45.103 27	−52.644 43	−60.174 92
SCF	−29.753 03	−37.218 14	−44.649 76	−52.103 88	−59.556 73
MP2	−29.801 45	−37.251 33	−44.726 09	−52.218 24	−59.688 84
G2MP2	−29.842 68	−37.302 29	−44.784 03	−52.272 83	−59.754 92
			Atomization Energy[b]		
B3LYP	54.4	72.4	95.5	130.3	149.6
SCF	15.5	36.3	35.5	49.0	61.3
MP2	44.2	55.3	81.5	110.8	141.3
G2MP2	71.4	88.6	119.7	155.2	186.5

[a] Using the 6-31G(d) basis set. [b] With zero-point energy corrections included.

TABLE 3: Enthalpies (kcal/mol) of Reactions for $BLi_n \rightarrow Li_n + B$[a]

level	SCF[a]	MP2[a]	G2MP2	B3LYP[a]
BLi_2 (C_{2v}, $^2B_2$)	33.5	32.7	31.8	36.4
BLi_3 (C_{2v})	18.9	60.7	63.1	62.0
BLi_4 (D_{2d})	47.8	67.1	86.7	79.9
BLi_5 (C_{4v})	40.6	123.4	110.2	105.0
BLi_6 (O_h)	87.7	121.9	122.4	128.0
BLi_7 (D_{5h})	68.2	132.7	120.4	118.9
BLi_8 (C_{3v})	76.7	101.7[b]		107.1

[a] Using the 6-31G(d) basis set and inclusion of zero-point energy (ZPE) corrections. [b] Without ZPE correction.

TABLE 4: Enthalpies (kcal/mol) of Reactions for $BLi_n \rightarrow BLi_{n-1} + Li$

level	SCF[a]	MP2[a]	G2MP2	B3LYP[a]
BLi ($^3\Pi_g$)	15.3	22.1	26.5	27.5
BLi_2 ($^2B_2$)	20.8	24.7	31.6	28.3
BLi_3 (C_{2v})	−6.2	34.8	43.4	37.0
BLi_4 (D_{2d})	33.4	29.8	56.6	41.5
BLi_5 (C_{4v})	13.5	67.3	40.7	43.1
BLi_6 (O_h)	46.4	24.7	43.3	46.2
BLi_7 (D_{5h})	-6.0	48.0	33.5	21.0
BLi_8 (C_{3v})	20.8	−10.3[b]		12.2

[a] Using the 6-31G(d) basis set and inclusion of zero-point energy (ZPE) corrections. [b] Without ZPE correction.

TABLE 5: Enthalpies (kcal/mol) of Reactions for $BLi_n \rightarrow BLi_{n-2} + Li_2$

level	SCF[a]	MP2[a]	G2MP2	B3LYP[a]
BLi_2 ($^2B_2$)	33.5	32.7	31.8	36.4
BLi_3 (C_{2v})	11.9	45.5	48.7	46.0
BLi_4 (D_{2d})	25.0	50.6	73.7	59.1
BLi_5 (C_{4v})	44.8	83.0	71.0	65.2
BLi_6 (O_h)	57.7	78.0	57.6	69.8
BLi_7 (D_{5h})	38.2	58.7	50.4	47.8
BLi_8 (C_{3v})	12.7	23.1[b]		13.9

[a] Using the 6-31G(d) basis set and inclusion of zero-point energy (ZPE) corrections. [b] Without ZPE correction.

hardly any energy difference with the C_{4h} and D_{4h} structures, indicating that BLi_4 has a very soft potential energy surface. Interestingly, at G2MP2 its D_{2d} form is 12.6 kcal/mol more stable than the C_{4v} isomer, while MP2 gives instead a reversed energetic preference of 13.2 kcal/mol. However, the energies obtained with these methods are influenced by high degrees of spin contamination, which is not the case at B3LYP. These observations suggests that the B3LYP method is well suited for analysis of the BLi_4 system. For convenience in comparing BLi_4 with the other BLi_n systems we consider the B3LYP D_{2d} structure as the global minimum.

The B3LYP cohesive energy of BLi_4 (D_{2d}) is 17.9 kcal/mol larger than that of BLi_3 and amounts to a sizable 79.9 or 20.0 kcal/mol per BLi interaction. Similar results are computed at

TABLE 6: Enthalpies (kcal/mol) of Reactions for $Li_n \rightarrow Li_{n-1} + Li$

level	SCF[a]	MP2[a]	G2MP2	B3LYP[a]
Li_2	2.1	14.0	26.3	19.4
Li_3 ($^2B_2$)	8.9	6.9	12.1	11.5
Li_4 (D_{2h})	4.4	23.4	33.0	23.5
Li_5 (C_{4v})	20.8	11.1	17.2	18.0
Li_6 (O_h)	−0.8	26.2	31.1	23.2
Li_7 (D_{5h})	13.5	41.0	35.5	30.0
Li_8 (T_d)	12.3	30.5	31.3	24.1

[a] Using the 6-31G(d) basis set.

TABLE 7: Enthalpies (kcal/mol) of Reactions for $Li_n \rightarrow Li_{n-2} + Li_2$

level	SCF[a]	MP2[a]	G2MP2	B3LYP[a]
Li_4 (D_{2h})	11.2	16.2	18.7	15.7
Li_5 (C_{4v})	23.1	20.4	23.8	22.1
Li_6 (O_h)	17.9	23.2	21.9	21.7
Li_7 (D_{5h})	10.6	41.5	40.2	33.8
Li_8 (T_d)	23.6	45.8	40.5	34.8

[a] Using the 6-31G(d) basis set.

G2MP2. BLi_4 has large endothermicities in the series of BLi_n clusters (vide infra) for both Li (41.5 kcal/mol) and Li_2 (59.1 kcal/mol) eliminations.

B. BLi_5. The C_{2v}, D_{3h}, and C_{4v} symmetry forms of hyperlithiated BLi_5 were studied (Figure 1). Meden et al.[8] reported earlier on the D_{3h} and C_{4v} forms at the SCF level. The C_{4v} structure is a minimum, while the 1.4 kcal/mol less stable D_{3h} form is a "hill-top" structure with two degenerate imaginary frequencies. Following one of its imaginary normal modes leads to the C_{2v} transition structure, which has an imaginary frequency of only 26i cm^{-1} at MP2 (67i cm^{-1} at SCF and 90i cm^{-1} at B3LYP). Tracing the B3LYP minimum energy path for this transition structure was unsatisfactory, since it led to a C_s form (not shown), which is only slightly distorted from C_{2v} symmetry and which also has an imaginary frequency (88i cm^{-1}). We were unable to trace the other minimum energy paths because of the flatness of the PES for BLi_5 of which the C_s, C_{2v}, and D_{3h} structures are separated by only 0.1 kcal/mol. For the BLi_5 (C_{4v}) minimum the axial B−Li distance of 2.163 Å is virtually identical to that of BLi_4 (D_{2d}); the equatorial B−Li distance (2.133 Å) is only slightly shorter. Note that coordination of lithium in BLi_5 prefers an open pyramidal arrangement while the most stable Li_5 form is planar.

Each of the five lithium atoms in BLi_5 is tightly coordinated to the boron atom; i.e., boron is hypercoordinated. The strength of these combined BLi interactions is reflected in the boron cohesive energy of 105.0 kcal/mol (or averaging 21.0 kcal/mol per BLi interaction), which is even 25 kcal/mol more than for BLi_4. Elimination of a single Li atom from the even-electron BLi_5 requires a significant 43.1 kcal/mol. It should be noted

that these reaction enthalpies are rather sensitive to the theoretical method employed. For example, the enthalpies alternate at the G2MP2 level of theory, and even more severely at both SCF and MP2, which is not surprising in light of the noted spin contamination obtained with these methods for BLi_4. Elimination of Li_2 from BLi_5 requires 65.2 kcal/mol, which is 6.1 kcal/mol more than for the corresponding process for BLi_4. For comparison, only 18.0 kcal/mol is required to dissociate a lithium atom from Li_5. Likewise, Li_2 elimination from Li_5 is 47.2 kcal/mol less endothermic than for BLi_5.

C. BLi_6. The O_h symmetry form is the only structure found for BLi_6. It is a minimum at all three levels of theory. Its B−Li bond distance of 2.145 Å (MP2) is somewhat shorter than those of the most stable BLi_4 (D_{2d}) and BLi_5 (C_{4v}) systems. The effect of electron correlation on the reduction of the B−Li distance by 0.074 Å is significant but smaller than the corresponding 0.21 Å found for the axial B−Li of BLi_5 (C_{4v}). BLi_6 has the largest cohesive energy (128.0 kcal/mol) of the BLi_n clusters. Li elimination (46.2 kcal/mol) is 31 kcal/mol more exothermic than for BLi_5, and Li_2 elimination (69.8 kcal/mol) requires 4.6 kcal/mol more than the corresponding process for BLi_5. For comparison, Li and Li_2 elimination from Li_6 (D_{3h}) requires "only" 23.2 and 21.7 kcal/mol, respectively. The BLi_6 cluster is predicted to be the most stable BLi_n cluster with respect to loss of Li and Li_2.

Positioning a boron atom inside a lithium cage, as in BLi_6, may be regarded as a first crude approximation of the energy of solvation for gaseous boron in the lithium melt.[8] The BLi_6 cohesive energy of 128.0 kcal/mol is then an estimate of the effect of the first solvation shell. The actual free energy of solvation is likely to be larger due to the entropy of mixing. Thus, on the basis of the 134.0 kcal/mol experimental cohesive energy of the boron crystal (but smaller values have also been reported),[26] the bulk lithium effect only needs to be ca. 6 kcal/mol to make B solvation in lithium a favorable process.

D. BLi_7. Three structures were identified for hyperlithiated BLi_7, one with D_{5h} symmetry and two with C_{3v} symmetry. The D_{5h} form is the most stable one. It represents a Li insertion in the Li_4 periphery of BLi_6, which accordingly lengthens the "equatorial" B−Li bond distance by 0.151 Å and the two "axial" B−Li bonds by only 0.027 Å. Capping one of the Li_3 faces of BLi_6 (O_h) with a Li atom leads to a C_{3v} form of BLi_7, which is 3.8 kcal/mol less stable than its D_{5h} isomer. This C_{3v} structure has a staggered conformation of the Li_3 and "tetrahedral" Li_4 units that are at opposite sites of the B atom. The barrier for rotation of the Li_3 plane around the principal axis leading to the C_{3v} eclipsed conformation (a transition structure) requires a significant 8.6 kcal/mol. Note that the C_{3v} structures have hexacoordinated borons.

With a coordination of seven, the boron−lithium cohesive energy has leveled off. This energy of 118.9 kcal/mol formally represents 17.0 kcal/mol per B−Li interaction versus 21.3 kcal/mol for the BLi_6 cluster. Accordingly, both Li and Li_2 eliminations also become significantly more facile compared to BLi_6 with respective reductions in reaction enthalpies of 24.8 and 22.0 kcal/mol. Note that it actually requires 9.0 kcal/mol less to dissociate a Li atom from BLi_7 than from Li_7. This highlights the special stability of BLi_6. However, the endothermicity of 47.8 kcal/mol for Li_2 elimination from BLi_7 is 14 kcal/mol larger than the corresponding endothermicity for Li_7.

E. BLi_8. Two structures with C_{3v} and D_{4h} point groups were identified. The most stable C_{3v} form can be viewed as Li-capping of the remaining Li_3 face of "staggered" BLi_7 (C_{3v}), which renders a structure in which two "tetrahedral" Li_4 units are bound by one boron atom. The boron is than formally hexalithiated. This C_{3v} structure is a minimum at both MP2 and B3LYP (albeit with a broken-symmetry solution) but has two imaginary frequencies at the SCF level. The symmetry of this odd-electron species deviates slightly from a D_{3d} form, as found for CLi_8,[7] because of the Jahn−Teller distortion. Comparison with the related BLi_7 (C_{3v}, eclipsed) shows that the additional Li cap in BLi_8 (C_{3v}) has little influence on the structural parameters, as might be expected.

The octalithiated boride structure (D_{4h}), in which the boron atom is located at the center of a Li_8 cube, is 26.6 kcal/mol less stable than the C_{3v} form at the SCF level. This structure has three imaginary frequencies and was not considered further also because of convergence problems at the correlated levels. We note that Meden at al.[8] reported an energy difference at SCF/6-31G(d) of 47.8 kcal/mol between the D_{4h} and C_{3v} structures.

Owing to limitations in resources, we obtained reaction enthalpies for BLi_8 (C_{3v}) only at B3LYP, which we discuss here, and at MP2 (excluding zero-point energy corrections). The cohesive energy of 107.1 kcal/mol has decreased compared to BLi_7 with 11.8 kcal/mol and compared to BLi_6 with 20.9 kcal/mol. The Li and Li_2 eliminations are also much less demanding (just as for BLi_7) and require at B3LYP only 12.2 and 13.9 kcal/mol, respectively. In contrast, the corresponding Li and Li_2 elimination from Li_8 require a significant 24.1 and 34.8 kcal/mol (same level), respectively. These are further indications that the hypercoordinated boron has become saturated with lithium atoms.

Conclusion

We examined structures and stabilities of the hyperlithated borides BLi_n ($n = 4-8$) at the SCF and correlated levels of theory. Inclusion of the effects of electron correlation is important in the characterization of stationary points, consistent with a previous study of the smaller borides BLi_n ($n = 1-3$). Fully hyperlithiated borides, up to BLi_7, are predicted to be stable. B3LYP cohesive energies of 79.9, 105.0, 128.0, and 118.9 kcal/mol were obtained for BLi_4, BLi_5, and BLi_6, and BLi_7, respectively. The most prominent hyperlithiated boride is BLi_6. The maximum Li coordination for boron is seven. Octalithiated boride with a boron atom surrounded by a cage of eight lithium atoms is not a minimum on the PES. Whereas the B3LYP and G2MP2 methods are in excellent agreement for the smaller lithium borides, differences of up to 15 kcal/mol are found for the larger systems. On the basis of cohesive energies and Li and Li_2 elimination reactions, B3LYP predicts BLi_6 to be the most stable cluster. G2MP2 on the other hand shows BLi_4 to have the highest endothermicities for loss of Li and Li_2. However, MCQDPT2 calculations for the BLi_4 system indicate that B3LYP gives more reliable results.

Acknowledgment. This work was supported in part by the Air Force Office of Scientific Research (Grant F49620-96-1-0450).

References and Notes

(1) Ivanic, J.; Marsden, C. J.; Hassett, D. M. *J. Chem. Soc., Chem. Commun.* **1993**, 822.

(2) Sannigrahi, A. B.; Kar, T.; Guha, N. B.; Hobza, P.; Schleyer, P. v. R. *Chem. Rev.* **1990**, *90*, 1061.

(3) Schleyer, P. v. R.; Würthwein, E.-U.; Kaufman, E.; Clark, T.; Pople, J. A. *J. Am. Chem. Soc.* **1983**, *105*, 5930.

(4) Cheng, H.-P.; Barnett, R. N.; Landman, U. *Phys. Rev. B* **1993**, *48*, 1820.

(5) Wu, C. H. *Chem. Phys. Lett.* **1987**, *139*, 357.

(6) Kudo, H. *Nature* **1992**, *355*, 432.

(7) Ivanic, J.; Marsden, C. J. *J. Am. Chem. Soc.* **1993**, *115*, 7503.
(8) Meden, A.; Mavri, J.; Bele, M.; Pejovnik, S. *J. Phys. Chem.* **1995**, *99*, 4252.
(9) Nguyen, K. A.; Lammertsma, K. *J. Phys. Chem. A* **1997**, *102*, 1608.
(10) Frisch, M. J.; Trucks, G. W.; Schlegel, H. B.; Gill, P. M. W.; Johnson, B. G.; Robb, M. A.; Cheeseman, J. R.; Keith, T.; Petersson, G. A.; Montgomery, J. A.; Raghavachari, K.; Al-Laham, M. A.; Zakrzewski, V. G.; Ortiz, J. V.; Cioslowski, J.; Stefanov, B. B.; Nanayakkara, A.; Challacombe, M.; Peng, C. Y.; Ayala, P. Y.; Chen, W.; Wong, M. W.; Andres, J. L.; Replogle, E. S.; Gomperts, R.; Martin, R. L.; Fox, D. J.; Binkley, J. S.; Defrees, D. J.; Baker, J.; Stewart, J. P.; Head-Gordon, M.; Gonzalez, C.; Pople, J. A. *GAUSSIAN94*, revision B.1; Gaussian, Inc.: Pittsburgh, 1994.
(11) Rothaan, C. C. J. *Rev. Mod. Phys.* **1951**, *23*, 69.
(12) Pople, J. A.; Nesbet, R. K. *J. Chem. Phys.* **1959**, *22*, 571.
(13) Pople, J. A.; Binkley, J. S.; Seeger, R. *Int. J. Quantum Chem. Symp.* **1976**, *10*, 1.
(14) Pople, J. A.; Krishnan, R.; Schlegel, B.; Binkley, J. S. *Int. J. Quantum Chem. Symp.* **1979**, *13*, 325.
(15) Kohn, W.; Sham, L. J. *Phys. Rev. A* **1965**, *140*, 1133.
(16) Hehre, W. J.; Ditchfield, R.; Pople, J. A. *J. Chem. Phys.* **1972**, *56*, 2257.
(17) Becke, A. D. *J. Chem. Phys.* **1993**, *98*, 5648.
(18) Becke, A. D. *Phys. Rev. A* **1988**, *38*, 3098.
(19) Lee, C.; Yang, W.; Parr, R. G. *Phys. Rev. B* **1988**, *37*, 785.
(20) Curtiss, L. A. R. K.; Pople, J. A. *J. Chem. Phys.* **1993**, *98*, 1293.
(21) Raghavachari, K.; Trucks, G. W.; Pople, J. A.; Replogle, E. S. *Chem. Phys. Lett.* **1989**, *158*, 207.
(22) Krishnan, R.; Binkley, J. S.; Seeger, R.; Pople, J. A. *J. Chem. Phys.* **1980**, *72*, 650.
(23) Curtiss, L. A.; Raghavachari, K.; Trucks, G. W.; Pople, J. A. *J. Chem. Phys.* **1991**, *94*, 7221.
(24) Schmidt, M. W.; Baldridge, K. K.; Boatz, J. A.; Elbert, S. T.; Gordon, M. S.; Jensen, J. J.; Koseki, S.; Matsunaga, M.; Nguyen, K. A.; Su, S.; Windus, T. L.; Dupuis, M.; Montgomery, J. A. *J. Comput. Chem.* **1993**, *14*, 1347.
(25) Nakano, H. *J. Chem. Phys.* **1993**, *99*, 7983.
(26) Kittel, C. *Introduction to Solid State Physics*, 6th ed.; Wiley: New York, 1986.